Systematic Onset of Periodic Patterns in Random Disk Packings

Nikola Topic,[1] Thorsten Pöschel,[1,2] and Jason A. C. Gallas[1,2,3]
[1]*Institute for Multiscale Simulation, Friedrich-Alexander-Universität Erlangen-Nürnberg, 91052 Erlangen, Germany*
[2]*Instituto de Altos Estudos da Paraíba, Rua Silvino Lopes 419-2502, 58039-190 João Pessoa, Brazil*
[3]*Complexity Sciences Center, 9225 Collins Avenue Suite 1208, Surfside, Florida 33154, USA*

(Received 6 July 2017; revised manuscript received 14 December 2017; published 5 April 2018)

We report evidence of a surprising systematic onset of periodic patterns in very tall piles of disks deposited randomly between rigid walls. Independently of the pile width, periodic structures are always observed in monodisperse deposits containing up to 10^7 disks. The probability density function of the lengths of disordered transient phases that precede the onset of periodicity displays an approximately exponential tail. These disordered transients may become very large when the channel width grows without bound. For narrow channels, the probability density of finding periodic patterns of a given period displays a series of discrete peaks, which, however, are washed out completely when the channel width grows.

DOI: 10.1103/PhysRevLett.120.148002

Introduction.—The problem of packing objects is very familiar both in real life and in several scientific disciplines. It defines an interesting class of optimization strategies whose primary goal is to bring as close as possible mono- or polydisperse objects with or without spatial confinement [1–7]. Packing is related to jamming in dynamical granular systems, being the subject of a large number of publications [8–10]. The ability to produce dense packings of particles allows one to minimize material porosity, a relevant feature, e.g., when sintering nanopowders used to engineer new materials having superior mechanical properties [11–13]. From a theoretical perspective, the optimal solution of packing problems is generically a NP-complete problem [14], namely, a task that cannot be solved in polynomial time in any way. This amounts to saying that packing objects is very hard for binary computers and that practical algorithms must rely on heuristics. The study of random packings of disks and spheres provides valuable insight for a variety of real-life complex systems [15,16].

In the last few years, we considered different aspects of packing problems. For instance, we found that very large three-dimensional heaps of particles display novel geometric characteristics involving internal and external angles of repose as well as distinct densities within the packing [17,18]. We also studied the structural defects present in large disks packings, showing the existence of a nonzero residual density of defects that obeys a power-law distribution as a function of the channel width [19].

The aim of this Letter is to report a remarkable result obtained from a systematic investigation of the pattern structure found in very large disks deposits formed by up to 10^7 disks, namely, for deposits much larger than the ones considered thus far in the literature. The startling finding is that, following a transient disordered phase, all deposits invariably become periodic. As described below, our systematic numerical simulations reveal that the probability density function of the transient lengths displays an approximately exponential tail. Furthermore, the probability density of finding periodic structures of a given period displays a series of discrete peaks that, however, are washed out completely when the channel width becomes large. This all means that disks packings become always asymptotically periodic after disordered transient phases, which, however, may be very large for wide channels.

Results.—Our large piles of monodisperse hard disks were obtained by randomly dropping disks of diameter d one by one into vertical channels of width w, measured in disk diameter d. The disks are confined by rigid walls, and are dropped vertically from initial positions x chosen randomly with a uniform probability distribution within the channel width. Typical examples of deposits are shown in Figs. 1 and 2. Additional examples are discussed in the Supplemental Material [20]. Disks piles were generated using the well-known ballistic deposition algorithm [15,17–19,21–25]. The implementation of this algorithm was described in detail elsewhere, in our previous study of the residual defect density in disk deposits [19].

Figure 1 illustrates a typical packing configuration observed near the bottom of the channel, i.e., before the onset of the final periodic pattern. As indicated in the figure caption, the colors encode the disk coordination number. Disregarding disks touching the ground and those located on the free surface, the average coordination number of a two-dimensional stable (static) packing is 4, represented in green in the figure. Such an average coordination number follows from the fact that each disk added to the sediment creates two new contacts when finding its stable position. Any disk having other than four contacts is considered a defect [19]. This definition is equivalent to definitions based on counting polygons made of neighboring bonds

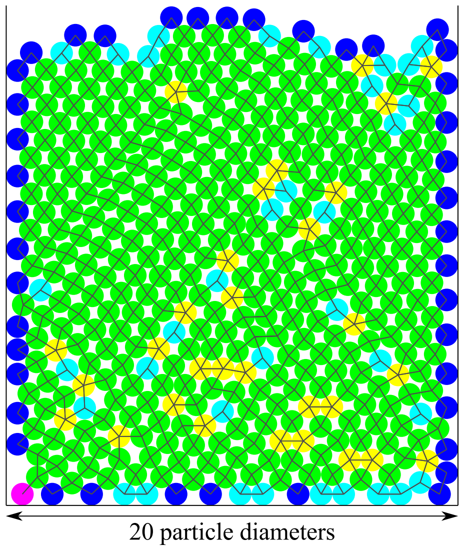

FIG. 1. A representative packing illustrating with colors the distribution of particle contacts. The particle with one contact is shown in purple, particles with two contacts in dark blue, three in cyan, four in green, and five in yellow. Vertical lines mark the limits of the channel. Bonds between particles are shown as line segments connecting their centers. Note the existence of voids (small white empty spaces).

different from a rhombus [21]. Thus, all disks not in green represent defects of the sediment. It is not difficult to realize that the existence or not of contacts and defects depends on the ordering of the sequential dropping during the transient.

The formation of a particle deposit depends on two distinct stages of the random dropping process. In an initial stage, the random dropping is responsible for fixing the random configuration of the bottom layer of the deposit, when particles are immobilized either after a direct vertical fall to the ground or, upon hitting a particle already at the bottom, by rolling over it until also hitting the ground, where both particles stay in contact. Since the dropping process is homogeneously distributed along the channel, particles on the bottom layer are not equally distributed. The bottom layer in Fig. 1 contains just 15 particles, out of 20 that could be fitted side by side on the bottom of the channel. The pile grows essentially in a row-by-row manner, with the bottom layer reflecting the specific random sequence of the initial dropping process. The particular distribution of particles in the bottom layer is very important for the subsequent growth process since it defines the network of local minima available for the subsequent particles to fall in while forming the packing.

The second stage of the sediment formation arises from the randomness involved in the specific ordering characteristic of the sequential dropping of successive layers that follow the formation of the bottom layer. Although the basal network of local minima is fixed by the bottom layer, the sequential order of the subsequent depositions is the key for shaping the final sediment. Its structure arises from the interplay of two mechanisms: the initial definition of the local stability minima by the bottom layer combined with the sequential order in which such minima are filled by falling particles. From the large number of possible minima available to form a particular pile once the bottom layer has been fixed, the effective minima selected are determined solely by the step-by-step randomness underlying the second stage of the sequential deposition process. Minute changes in the initial creation and/or in the subsequent selection of the minima network will drastically change the final structure of the deposit.

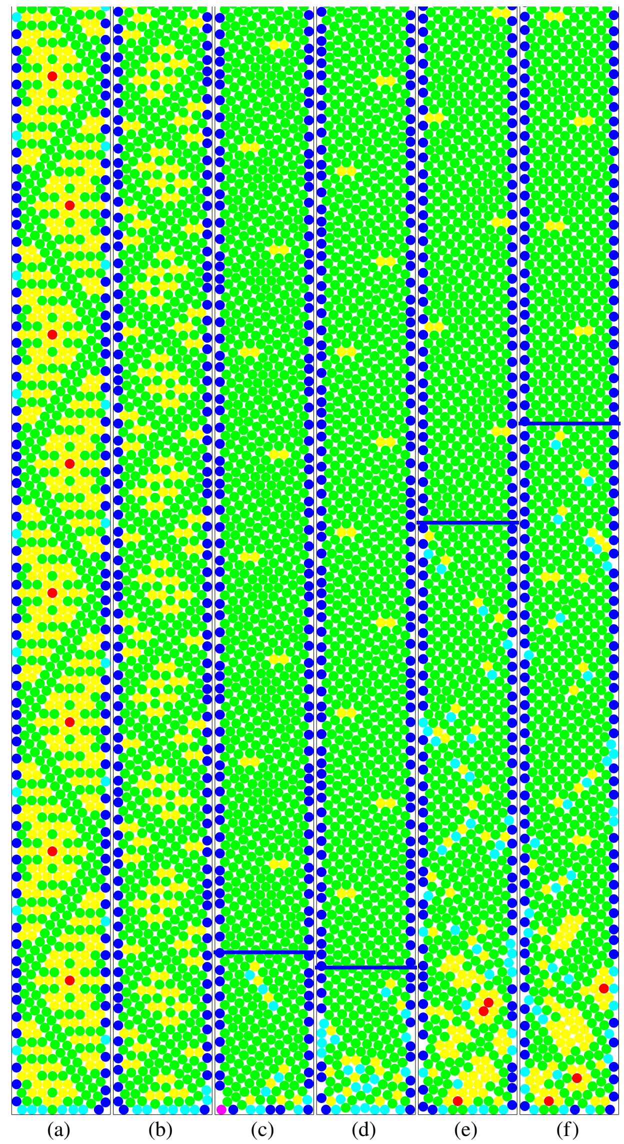

FIG. 2. Six typical packings obtained for distinct random initial configurations. Following an initial transient, one sees the onset of a periodic pattern (indicated by horizontal line segments, when not periodic from the start). The channel width is $w = 10$ particle diameters and the height h is about $10w$. For small widths, transients can be rather small. Also visible are the transient and the periodic structures of voids (white empty spaces). Particles with six contacts are shown in red.

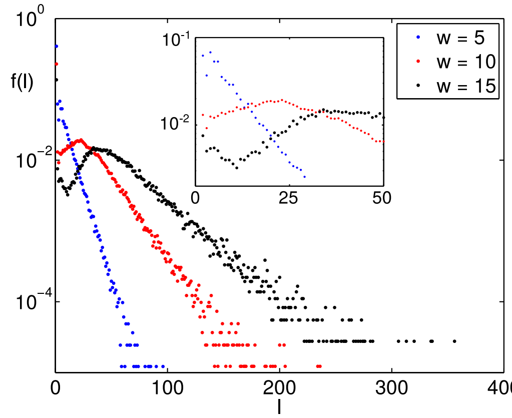

FIG. 3. Typical probability density functions of having a transient length ℓ, plotted for three distinct values of the channel width w. Sample sizes: 80 000 for $w = 5$ and 10, and 36 000 for $w = 15$. Collapsed plots are given in the Supplemental Material [20].

Figure 2 shows examples of the complete packing structure found along a small width channel, chosen for better visibility. Each channel illustrates both the initial irregular transient structure and the asymptotic periodic pattern. From these examples we recognize that transients decay relatively fast with the deposit height. Noteworthy, however, is the fact that there is a consistent onset of a periodic structure subsequent to the transient regime. This was found to be true for all deposits investigated. In other words, independently of the randomness of the deposition, we consistently find a periodic structure to emerge after a transient stage.

One may find two types of patterns in the channels. As illustrated in Figs. 2(a) and 2(b), patterns of the simplest type are those where the packing is periodic from the very start of the deposition. In the second type, exemplified by Figs. 2(c)–2(f), the packing becomes periodic only after an initial irregular transient growth that can be relatively long [Fig. 2(f)]. Figure 2 shows defects to be regularly spread along the channel and to be traceable by performing simple translations along the channel. Asymptotically, the channel is tiled by periodic patterns, mosaics, which, except for some exceptional very symmetrical initial conditions, always contain defects embedded in them [19].

How can we characterize the average length of the transients needed for particle configurations inside the channel to become periodic? To this end, for a fixed width we measured the transient lengths ℓ for n independent deposits as indicated in the figure caption. Then, each histogram is obtained by simple binning: $f(\ell)$ gives the fraction of transients within $[\ell - \Delta\ell/2, \ell + \Delta\ell/2]$ divided by $\Delta\ell$. Here, we performed averages over independent deposits, for the sampling sizes indicated in the figure caption. Figure 3 shows the results obtained for three widths, $w = 5$, 10, and 15. From this figure we see that larger widths imply longer transients. But the important fact here is that the transients are always finite. Figure 4 displays plots similar to the ones in Fig. 3, but for larger values of w, namely, for $w = 50$ and 250.

Figure 4 contains small line segments providing estimates for the exponent tails, assuming them to be exponential: $f(\ell) = \text{constant} \times \exp(k\ell)$. Explicitly, we find $k = -0.05 \pm 0.01$ for $w = 10$, $k = -0.007 \pm 0.001$ for $w = 50$, and $k = -(2.4 \pm 0.6) \times 10^{-3}$ for $w = 250$. Error bars were estimated by splitting the x coordinate range covered by the red segments into five equal segments, and then fitting the slope for each segment. The error was the maximal deviation from the mean for those five segments. For $w = 250$ we used only three segments, because fluctuations are bigger than the mean.

Figure 5 shows the distribution $g(a)$ of the periods, a, for three channel widths w. In this figure, for bins of width Δa centered at a, $g(a)\Delta a$ gives the fraction of periods belonging to interval $[a - \Delta a/2, a + \Delta a/2]$. Conspicuously, while the distribution looks discrete for very narrow channels [22], such as $w = 10$ [Fig. 5(a)], discreteness is washed out when w increases [Fig. 5(c)]. Magnifications of the horizontal scale do not show any sign of discreteness for $w = 250$.

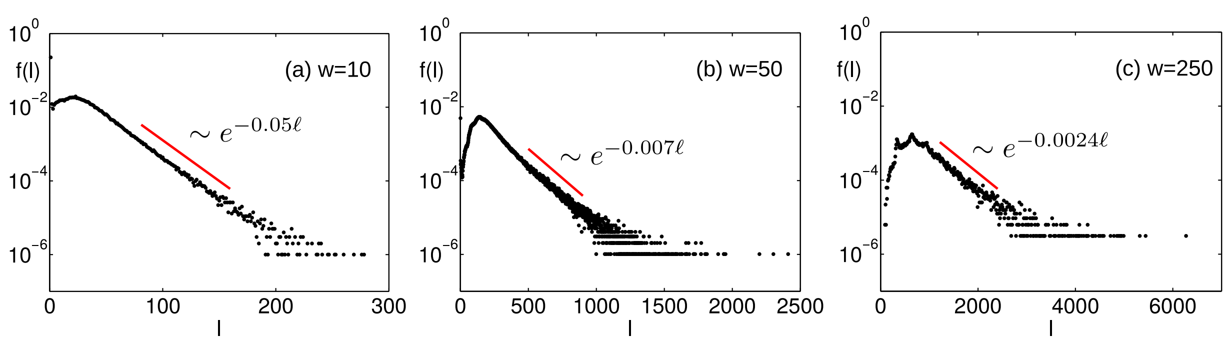

FIG. 4. Same probability distributions as in Fig. 3, but for channel widths $w = 10$, 50, and 250 and averaging over larger samples. The plot for $w = 10$, distinct from the one in Fig. 3, is given to facilitate comparisons. Sample sizes: 10^6 for $w = 10$, 8×10^5 for $w = 50$, and 19×10^3 for $w = 250$. As indicated by the line segments in the panels, the tails seem to obey exponential laws. Collapsed plots are given in the Supplemental Material [20].

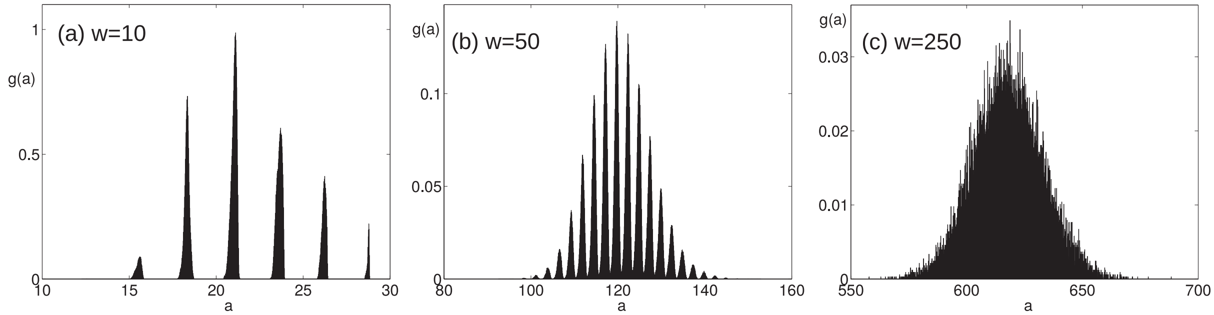

FIG. 5. Distributions $g(a)$ of periods a for $w = 10$, 30, and 250. Here, for bins of width Δa centered at a, $g(a)\Delta a$ gives the fraction of periods belonging to the interval $[a - \Delta a/2, a + \Delta a/2]$. The number of bins in the range from the minimal to the maximal existing period on each figure is 1000. Panels (a), (b), and (c) are calculated for 1 000 000, 800 000, and 25 000 system realizations, respectively.

As a final experiment, Figs. 6 illustrates the evolution of the distribution of periods as a function of the channel width w. The leftmost panel shows behaviors for $w \leq 30$ while in the rightmost panels one sees what happens for larger widths, near $w = 300$. The distribution $g(a)$ of periods no longer depends on the channel width for channel widths $200 \leq w \leq 300$. The trend displayed in Fig. 6 shows no sign that the transition to periodicity ceases to exist for larger values of w, i.e., in other words, that it always becomes periodic, independently of the width. That this is indeed plausible follows from the fact that by fixing the bottom layer one simultaneously fixes the network of local minima available for subsequent particles to fall in. For any finite width w, the number of local minima available is always finite and, eventually, the sequence of fillings is bound to repeat. Additional numerical experiments are described in the Supplemental Material [20].

Conclusions.—In summary, we investigated properties of large deposits of disks constrained by hard walls (complementary aspects, observed under periodic boundary conditions, were studied before [19]). Compelling evidence was found that, independently of the width of the channels, all packings eventually become periodic. In the literature, there are reports of cases of periodic disks piles observed in narrow channels [22,23]. Here, however, the new twist is that, instead of isolated periodic configurations, we find *every* pile to eventually become periodic, independently of the channel width. In this context, we recall work based on the theoretical considerations of some local disks configurations that presented arguments supporting asymptotic periodicity in the narrow channel limit, under a number of restrictive hypotheses [26]. While we are not able to prove that every pile must be periodic, in our extensive simulations involving the deposition of up to 10^7 disks, we never found a nonperiodic pattern. It would be interesting to study, as a function of the channel width, the combinatorial problem of determining the number of network minima available for piles to grow and to see if the generic problem allows one to demonstrate the existence of periodicity for all cases. The particles considered in this article have equal diameters; however, it would be also of interest to study systems of polydisperse particles, because small amounts of polydispersity are always present in experimental realizations of particulate systems. Further suggestions for future work include to study different system boundaries and to consider extensions to three dimensions.

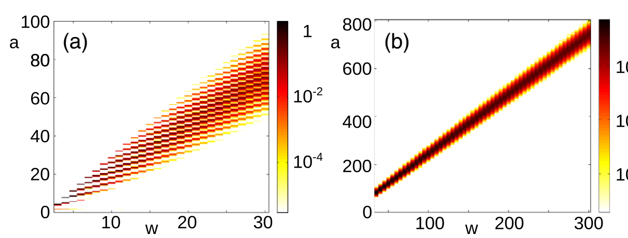

FIG. 6. Evolution of the distribution $g(a)$ of periods represented in colors as a function of the period a and channel width w. (a) For channel widths $w = 3, 4, \ldots, 30$, the distribution $g(a)$ is calculated in 300 bins spanning the periods $0 < a < 100$. (b) The channel widths are $w = 35, 40, 45, \ldots, 300$, and for each w the 300 bins span the range $0 < a < 800$.

The authors gratefully acknowledge the support of the Cluster of Excellence Engineering of Advanced Materials, ZISC and FPS funded by the German Research Foundation (DFG). J. A. C. G. was supported by Conselho Nacional de Desenvolvimento Científico e Tecnológico, Brazil.

[1] S. Torquato, *Random Heterogeneous Materials: Microstructure and Macroscopic Properties*, (Springer, Berlin, 2002).
[2] A. Lodi, S. Martello, and M. Monaci, Two-dimensional packing problems: A survey, Eur. J. Oper. Res. **141**, 241 (2002).
[3] T. Aste and D. Weaire, *The Pursuit of Perfect Packing* (Institute of Physics, London, 2000).
[4] P. Meakin and A. T. Skjeltorp, *Application of Experimental and Numerical Models to the Physics of Multiparticle Systems*, Advances in Physics, Vol. 42, (Taylor and Francis, Oxford, 1993).
[5] F. Delyon and Y. E. Levy, Instability of 2d random gravitational packings of identical hard spheres, J. Phys. A **23**, 4471 (1990).

[6] J. G. Berryman, Random close packing of hard spheres and disks, Phys. Rev. A **27**, 1053 (1983).

[7] See K. W. Wojciechowski, P. Pieranski, and J. Malecki, An instability in a hard-disk system in a narrow box, J. Phys. A **16**, 2197 (1983), and references therein.

[8] E. I. Corwin, H. M. Jaeger, and S. R. Nagel, Structural signature of jamming in granular media, Nature (London) **435**, 1075 (2005).

[9] D. Bi, J. Zhang, B. Chakraborty, and R. P. Behringer, Jamming by shear, Nature (London) **480**, 355 (2011).

[10] C. P. Goodrich, S. Dagois-Bohy, B. P. Tighe, M. van Hecke, A. J. Liu, and S. R. Nagel, Jamming in finite systems: Stability, anisotropy, fluctuations, and scaling, Phys. Rev. E **90**, 022138 (2014).

[11] D. Lahiri, V. Singh, G. R. Rodrigues, T. M. H. Costa, M. R. Gallas, S. R. Bakshi, S. Seal, and A. Agarwal, Ultrahigh-pressure consolidation and deformation of tantalum carbide at ambient and high temperatures, Acta Mater. **61**, 4001 (2013).

[12] A. Mesquita, M. I. B. Bernardi, V. R. Mastelaro, M. H. Lente, J. A. Eiras, M. R. Gallas, and T. M. H. Costa, Nanograined ferroelectric ceramics prepared by high-pressure densification technique, J. Am. Ceram. Soc. **92**, 1679 (2009).

[13] X. Jia, N. Gopinathan, and R. A. Williams, Modeling complex packing structures and their thermal properties, Adv. Powder Tech. **13**, 55 (2002).

[14] M. Garey and D. Johnson, *Computers and Intractability: A Guide to the Theory of NP-Completeness* (W. H. Freeman, New York, 1979).

[15] N. Topic and T. Pöschel, Steepest descent ballistic deposition of complex shaped particles, J. Comput. Phys. **308**, 421 (2016).

[16] H. M. Harreis, M. Schmidt, and H. Löwen, Decoration lattices of colloids adsorbed on stripe-patterned substrates, Phys. Rev. E **65**, 041602 (2002).

[17] N. Topic, J. A. C. Gallas, and T. Pöschel, Nonuniformities in the Angle of Repose and Packing Fraction of Large Heaps of Particles, Phys. Rev. Lett. **109**, 128001 (2012).

[18] N. Topic, J. A. C. Gallas, and T. Pöschel, Characteristics of large 3d heaps of particles produced by ballistic deposition from extended sources, Philos. Mag. **93**, 4090 (2013).

[19] N. Topic, T. Pöschel, and J. A. C. Gallas, Residual defect density in random deposits of disks, Sci. Rep. **5**, 12703 (2015).

[20] See Supplemental Material at http://link.aps.org/supplemental/10.1103/PhysRevLett.120.148002 for additional plots and complementary experiments.

[21] P. Meakin and R. Jullien, Two-dimensional defect-free random packing, Europhys. Lett. **14**, 667 (1991).

[22] P. Meakin and R. Jullien, Periodic disc packings generated by random deposition in narrow channels, Europhys. Lett. **15**, 851 (1991).

[23] R. Jullien and P. Meakin, Computer simulations of steepest descend ballistic depositions, Colloids Surf. A **165**, 405 (2000).

[24] W. M. Visscher and M. Bolsterli, Random packing of equal and unequal spheres in two and three dimensions, Nature (London) **239**, 504 (1972).

[25] A. Higgins, Hard sphere packing on an inclined plane, J. Phys. A **29**, 2373 (1996).

[26] J. E. S. Socolar, Theory of packing of identical hard disks generated by ballistic deposition, Europhys. Lett. **18**, 39 (1992).